INVESTIGATION OF CRACK TIP DISPLACEMENT IN POLYTETRAFLUOROETHYLENE USING FULL-FIELD METHOD

L.C.S. Nunes, luizcsn@mec.uff.br
Laboratory of Opto-Mechanics (LOM/LMTA), Department of Mechanical Engineering (TEM/PGMEC), Universidade Federal Fluminense, Rua Passo da Pátria, 156, Bloco E, Niteroi-RJ, CEP: 24210-240, Brazil.

Abstract. The main purpose of the present paper is to analyze the crack opening displacements and craze zone at the crack tip in polytetrafluoroethylene (PTFE) by means of full-field displacement method. In order to do this, an uniaxial tensile test is performed using a double-edge-cracked plate specimen of PTFE. The experimental procedure is conducted with digital image correlation method, which is an available optical-numerical method developed to determine displacement fields. Moreover, a mathematical model based on linear elastic fracture mechanic (LEFM) is proposed, in which the coefficients are estimated by means of nonlinear least-squares fitting method. The aim is to investigate an alternative expression to predict displacements around crack of materials that present nonlinear behavior.

Keywords: *Crack opening displacement, Polytetrafluoroethylene, Polymer, digital image correlation.*

1. INTRODUCTION

Polymer characterization has been extensively studied in recent years. This is mainly because the complexity of polymer response. There are several types of polymers, which can have different characteristics. Polytetrafluoroethylene (PTFE) constitutes a commercially important class of available polymers, in which is characterized by high melting point, very good resistance against chemicals and extremely low friction. Therefore, it is being used in a large number of applications such as bearings, pipes, sealing rings and electrical insulation.

Analyses of compressive and tensile response of PTFE at differing strain-rates and temperatures have been developed in the literature (Rae and Dattelbaum, 2004; Rae and Brown, 2005; Bergström and Hilbert, 2005). With these studies, some mechanical parameters of PTFE have been identified. For this purpose, all experimental data were obtained from standard test methods.

In order to improve standard tests, full-field optical methods have emerged as practical tools in the experimental mechanics (Dally and Riley, 2005; Sharpe, 2008). Among these methods, digital image correlation (DIC) is one of the most commonly investigated and improved in the last years (Poissant and Barthelat, 2010; Triconnet et al., 2009; Huang et al., 2010; Pan et al., 2009; Zhang et al., 2011; Lava et al., 2010, 2011). The DIC is an optical-numerical method developed for evaluating displacement fields. Its special merits encompass non-contact measurements, simple optic setups, no special preparation of specimens and no special illumination.

Nowadays, various methodologies have been developed using DIC method to estimate physical properties and describe mechanical behavior of some materials (Avril et al., 2008; Guélon et al., 2009; Dournaux et al., 2009; Nunes, 2011). Some of these studies are conducted on crack tip fields, where, most of them are mainly focused on the stress intensity factors and crack tip opening (Yoneyama et al., 2007; Roux et al., 2009; Yates et al., 2010; Chen et al., 2010).

The purpose of this work is to investigate the crack opening displacements and craze zone at the crack tip in polytetrafluoroethylene (PTFE) through a single specimen. The experimental testing was performed in quasi-static condition and at room temperature. In this testing, a double-edge-cracked plate specimen was subjected a tensile load. Moreover, the displacement fields from a region around the crack tip were estimated by means of DIC method. In order to predict these behaviors a mathematical model based on linear elastic fracture mechanic is proposed.

2. FIELD EQUATIONS FOR THE REGION NEAR TO CRACK TIP

In the present work, a double-edge-cracked plate specimen under tensile load is taken into consideration, as shown in Fig. 1(a). Figure 1(b) illustrates the crack tip system and notation for field components around the crack, which may be written in terms of the polar coordinates centered at the crack tip. The displacement and deformation fields, which is associated with vertical component, near to the crack tip for plane stress conditions assuming a homogeneous, isotropic and linearly elastic solid and opening mode I (LEFM), may be expressed in the following form (Dally and Riley, 2005; Gdoutos, EE, 2005),

$$u(r,\theta) = \frac{K_I}{\mu\sqrt{2\pi}}\sqrt{r}\sin\frac{\theta}{2}\left(\frac{2}{1+\nu} - \cos^2\frac{\theta}{2}\right) \quad (1)$$

$$\varepsilon_x(r,\theta) = \frac{K_I}{E\sqrt{2\pi}}\frac{1}{\sqrt{r}}\cos\frac{\theta}{2}\left[(1-\nu)+(1+\nu)\sin\frac{\theta}{2}\sin\frac{3\theta}{2}\right] \tag{2}$$

Herein, the shear modulus is given by $\mu = \frac{E}{2(1+\nu)}$, where E is the modulus of elasticity and ν is the Poisson's ratio.

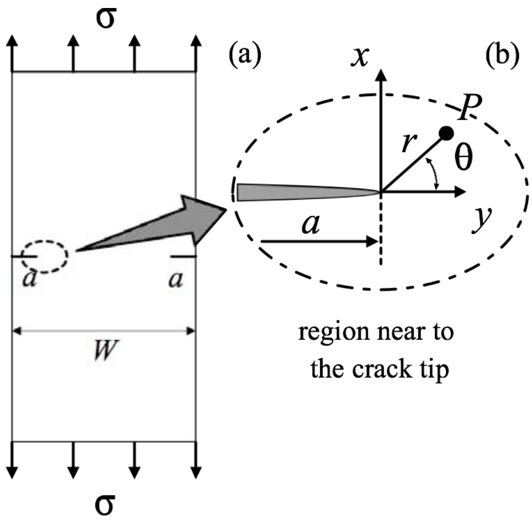

Figure 1. (a) Schematic illustration of the double-edge-cracked plate subjected to tensile load; (b) coordinates defined with the origin at the crack tip.

For geometrical shape, as shown in Fig 1(a), the opening mode stress intensity factor K_I depends linearly on the applied load σ and is a function of the crack length a and the geometry of the cracked specimen. In the present case, the stress intensity factor for a double-edge-cracked plate specimen (see Fig. 1(a)) is defined by (Gdoutos, EE, 2005).

$$K_I = \sigma\sqrt{\pi a}\left[1.12 - 0.2\left(\frac{a}{W}\right) - 1.2\left(\frac{a}{W}\right)^2 + 1.93\left(\frac{a}{W}\right)^3\right] \quad 0 < \frac{a}{W} < 0.7 \tag{3}$$

3. EXPERIMENTAL SET-UP

3.1. Material and specimen

The specimen was made of polytetrafluoroethylene (PTFE). The geometrical shape for a double-edge-cracked plate specimen, schematically illustrated in Fig. 1, was considered with the following data: crack length, a, equal to 3.0 mm; width of plate, W, equal to 25 mm; thickness of plate, t, equal to 2 mm and the length of plate was equal to 250 mm. In present analysis, r and θ express the polar coordinates around a crack tip as illustrated in Fig. 1. Moreover, region of analysis, which was taken near the crack tip, is also indicated.

3.2. Digital image correlation

Digital image correlation (DIC) method has been considerably improved and its principle is well known. In this way, the aim of this section is to present a brief description of the DIC method, which is well documented in the literature. The basic principle of the DIC method is to match maximum correlation between small zones (or subsets) of the specimen, which is coated by a random pattern, in the undeformed and deformed states. The image correlation is performed by comparing subsets from reference image with subsets from each of the deformed images. The schematic diagram is illustrated in Fig. 2. From a given image-matching procedure, the displacement fields, or displacement at different positions, in the analysis region can be computed. For this purpose, the minimization of the correlation coefficient is taken into account, which provides the in-plane displacement fields designated by $u(x,y)$ and $v(x,y)$. A commonly used correlation coefficient is defined as follows,

$$c(u,v) = \frac{\sum_{i=1}^{m}\sum_{j=1}^{n}\left[f(x_i,y_j)-\bar{f}\right]\left[g(x'_i,y'_j)-\bar{g}\right]}{\sqrt{\sum_{i=1}^{m}\sum_{j=1}^{n}\left[f(x_i,y_j)-\bar{f}\right]^2}\sqrt{\sum_{i=1}^{m}\sum_{j=1}^{n}\left[g(x'_i,y'_j)-\bar{g}\right]^2}} \tag{4}$$

$$\begin{aligned} x' &= x + u_0 + \frac{\partial u}{\partial x}dx + \frac{\partial u}{\partial y}dy \\ y' &= y + v_0 + \frac{\partial v}{\partial x}dx + \frac{\partial v}{\partial y}dy \end{aligned} \tag{5}$$

where $f(x,y)$ is the pixel gray level value (ranging from 0 to 255) at the coordinates (x,y), for the undeformed image; $g(x',y')$ is the pixel gray level value at the coordinates (x',y') for the deformed image; $\bar{f}$ and $\bar{g}$ are the average gray values for images and, finally, *u* and *v* are, respectively, the displacement components for the subset centers in the *x* and *y* directions.

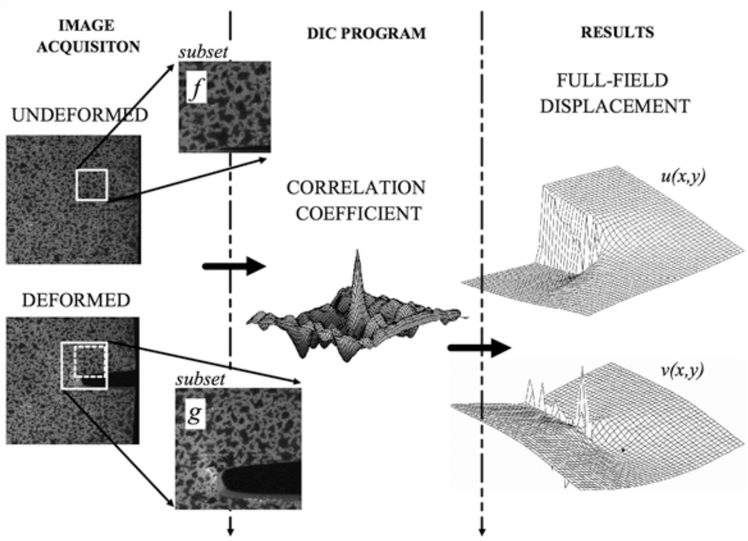

Figure 2. Scheme of digital image correlation method

3.3. Experimental arrangement

The experimental arrangement for conducting tension testing involves an apparatus developed to apply load in a double-edge-cracked plate specimen, a CCD camera set perpendicularly to the specimen and a computer for capturing and processing the images, as shown in Fig. 3. The specimen in the load apparatus was covered with painted speckles (random black and white pattern) to provide a grayscale distribution with sufficient contrast, which can be tracked from image, thus improving the matching procedure. It is in agreement with the geometrical model, as seen in Fig. 1. The CCD camera (Sony XCD-SX910) used to record the images of the specimen has a resolution of 1376x1024 pixels. In this experimental configuration, one pixel of the CCD camera corresponds to an area approximately equal to 4.65×4.65 μm^2 on the specimen.

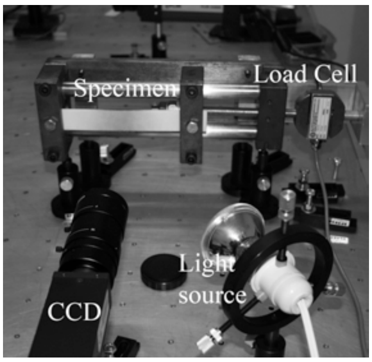

Figure 3.Experimental set-up

For determining the displacement fields, the specimen was subjected to two different loads, which are associated with undeformed and deformed states. The images of the undeformed and deformed specimen were captured and processed using DIC program, in which its basic principle is described in section 3.2. The procedure was conducted in quasi-static conditions at room temperature. In this condition, there are no effects of machine vibrations. It is important to emphasize that the undeformed state was associated with zero load.

4. RESULTS AND DISCUSSION

In order to investigate the crack behavior, a small region near to crack tip is selected. In Figure 4, a set of images associated to different applied loads (0, 89, 194, 304, 400, 455, 485 and 500 N) is illustrated. It can be note that the crack is opening with applied load, however evident propagation is not observed.

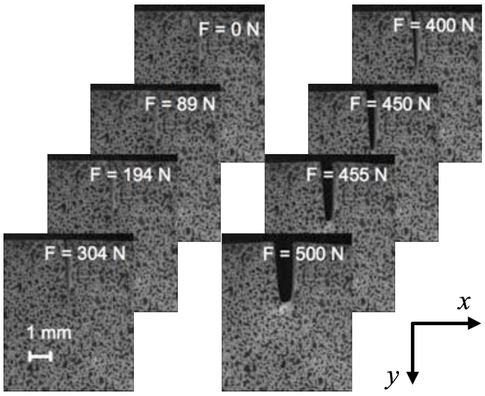

Figure 4. Region around the crack tip: crack open for different applied loads.

By using the DIC program, which principle is previously described in section 3.2, full-field *u* and *v*-displacements are obtained. The *u*-displacement is associated with *x*-coordinate, i.e., crack opening direction. Furthermore, *v*-displacement is associated with *y*-coordinate. Figures 5 and 6 show three-dimensional displacement profiles for applied loads equal to 89, 304, 450 and 500N. In both data sets, it is observed the crack opening, mainly at *u*-displacement.

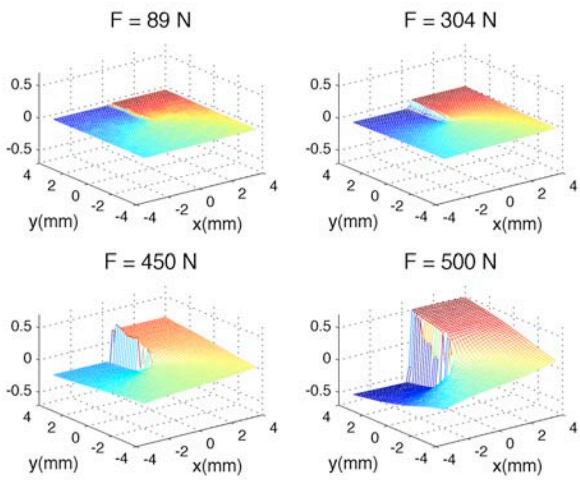

Figure 5. Three-dimensional *u*-displacement profile for different applied loads.

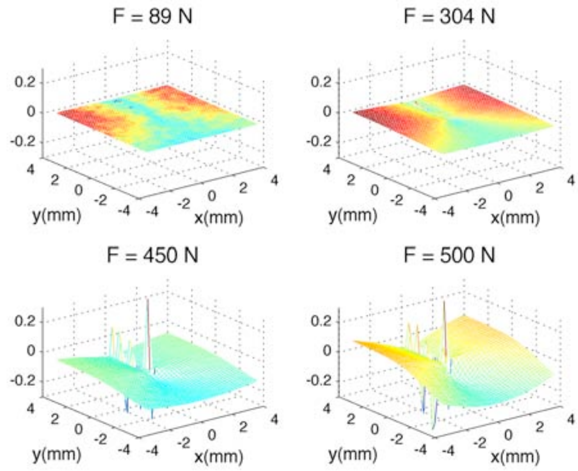

Figure 6. Three-dimensional *v*-displacement profile for different applied loads.

In the present analysis, the focus is to investigate the crack opening displacement. In this purpose, only *u*-displacements are taken into account. The Schematic of *u*-displacement considering from a crack with craze zone is shown in Fig. 7. In this scheme, the region of analysis may be divided in two parts, one of them is related to displacement of crack opening, which is designed by δ (half size of total displacement) and has a length equal to initial crack a, and the other is the deformation (or craze zone) that has a length of r_p.

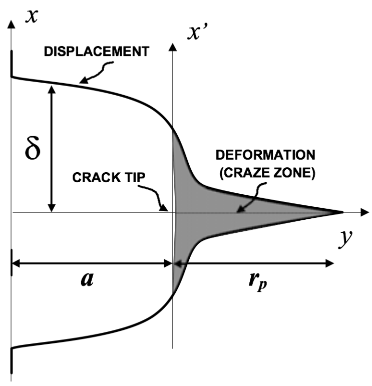

Figure 7. Schematic of a crack tip with the craze zone.

Figure 8(a) illustrates *u*-displacement for different applied loads obtained by means of DIC method. These results are measured at center of crack. As a means to estimate the length of crack for each applied load, the slope of the curve of displacement versus *y*-coordinate was taken. In figure 8(b), the maximum value of slope, which is related with inflection point, is assumed as the crack-tip.

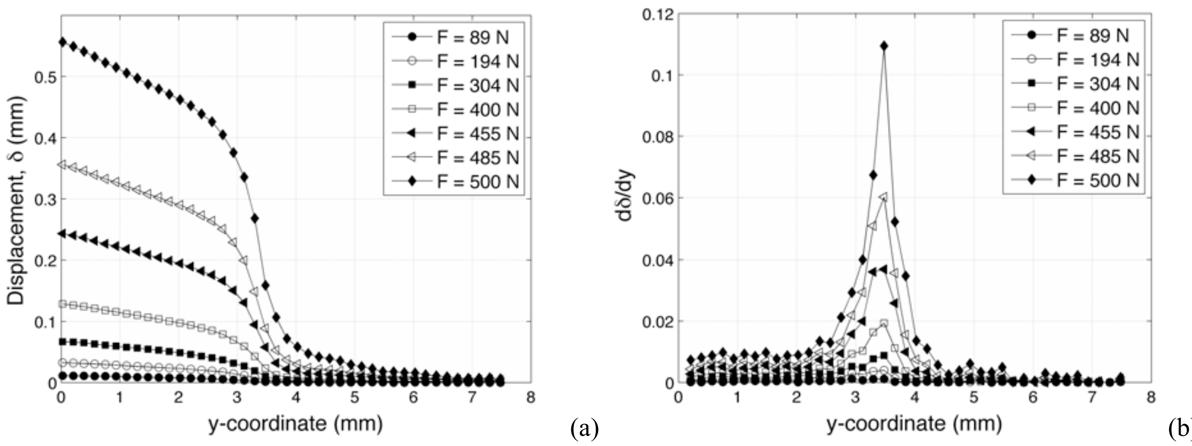

Figure 8. (a) Experimental measured displacement profile of crack and (b) differentiation for estimating crack length.

The results of crack length for different applied loads obtained from described procedure are shown in Table 1. In addiction, the stress associated to loads is calculated considering the geometry of specimen (thickness x width = 2 x 25 mm^2) presented in section 3.1.

Table 1. Crack length for different applied loads.

Applied load, F (N)	Stress (MPa)	Crack length, *a*(mm)
89	1.75	2.93
194	3.82	3.16
304	5.98	3.22
400	7.87	3.33
455	8.96	3.37
485	9.55	3.39
500	9.84	3.43

Now, for finding a mathematical expression that describes the experimental data from a crack displacement, LEFM is taken into consideration. Taking Eqs. (1) and (2), considering the angle equal to 180 degree for *u*-displacement and 0 degree for deformation. Moreover, three coefficients are added to initial expression: w_0, u_0 and ε_0 are related to rotation and translations, respectively. These parameters were included to correct experimental errors.

$$u(r) = \frac{4K_I}{E\sqrt{2\pi}}\sqrt{r} + w_0 r + u_0 \text{ for } \theta = 180^o \tag{6}$$

$$\varepsilon_x(r) = \frac{K_I}{E\sqrt{2\pi}}\frac{1}{\sqrt{r}}(1-\nu) + \varepsilon_0 \text{ for } \theta = 0^o \tag{7}$$

By Eqs. (6) and (7), the following expression is considered,

$$\delta = \begin{cases} C_1\sqrt{|y|} + w_0 y + u_0, \; for \; -a < y < 0 \; (displacement \;\; region) \\ \dfrac{C_2}{\sqrt{|y+a|}} + \varepsilon_0, \; for \;\; 0 > y > a \; (deformation \;\; region - craze \;\; zone) \end{cases} \tag{8}$$

where C_1, C_2, w_0, u_0 and ε_0 are coefficients to be determined, and *a* are different crack lengths that were estimated and their values are shown in Table 1. By fitting Eq. (8) to the experimental data of *u*-displacement, these coefficients may be estimated. This procedure was performed using nonlinear least-squares fitting method. Figure 9 shows the experimental data and fitted model (Eq. (8)) for two parts, i.e., displacements from crack side and craze zone.

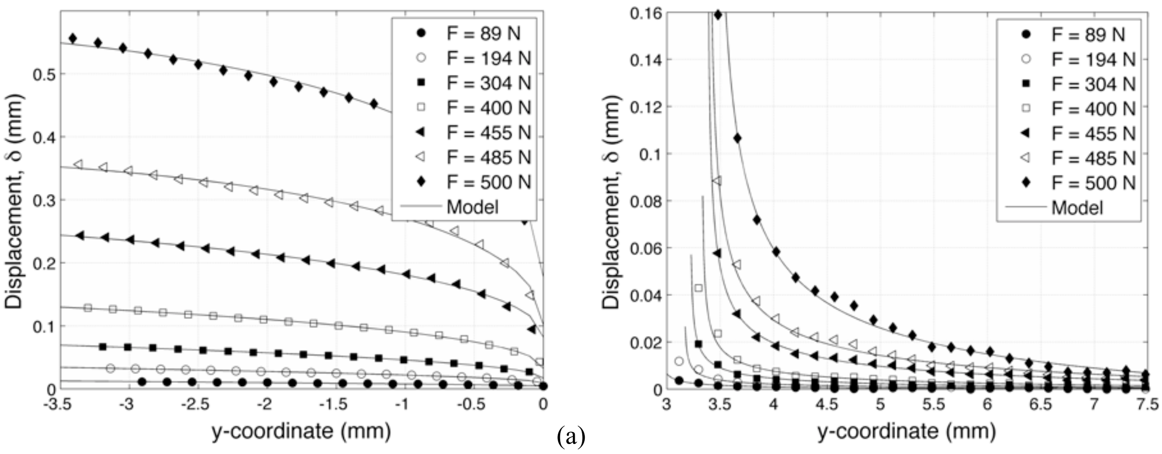

(a) (b)

Figure 9. Comparison of experimental measured and fitted model: (a) Displacement from crack side and (b) displacement from craze zone.

It can be clearly seen that the fitted model are closer to the experimental data. Firstly, the influence of coefficients C_1 and C_2 as a function of applied loads are investigated. These coefficients are related with the first terms of linear elastically fracture mechanics (see Eq. (6)). The associated results are plotted in Fig 10. In this analysis, the data for opening mode stress intensity factor (see Eq. (1)) were taken from section 3.1; Young's modulus and Poisson ratio are assumed equal to 0.46 MPa and 0.44 respectively (Nunes, 2011).

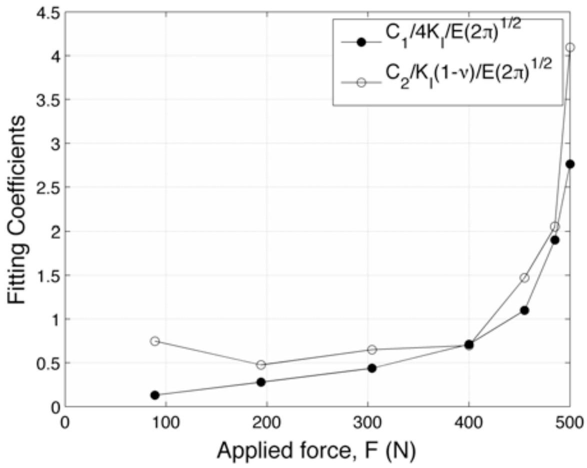

Figure 10. Behavior of fitting coefficients, C_1 and C_2.

By analyzing the values of $C_1 \Big/ \dfrac{4K_I}{E\sqrt{2\pi}}$ and $C_2 \Big/ \dfrac{K_I(1-\nu)}{E\sqrt{2\pi}}$, it is possible to observe that both terms present same behavior when different loads are applied. Therefore, the choice of Eq. (8) in association with Eq. (7) may be acceptable (for instance).

The coefficients w_0, u_0 and ε_0, which are experimentally associated with rotation and displacements, as a function of applied loads are illustrated in Fig. 11. For values of applied forces larger to 400 N the coefficient values increase considerably.

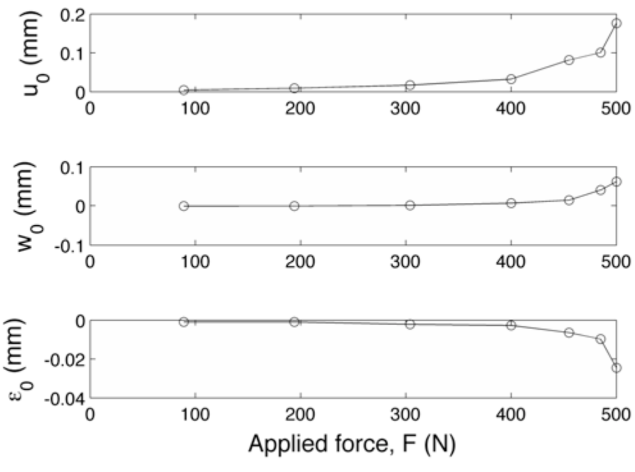

Figure 11. Coefficients associated with applied forces: u_0 and ε_0 rigid translation; w_0 rotation.

The increase of the crack-tip-opening displacements (CTOD) for different applied loads and associated crack extension are show in Fig 12. By results, it can be noted the non-linear increase of CTOD with applied force.

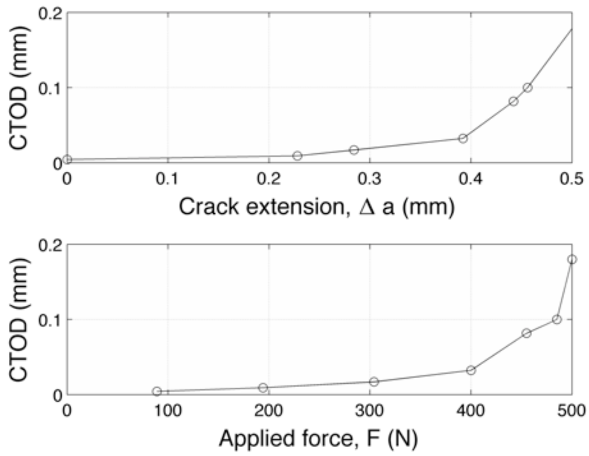

Figure 12. Crack-tip-opening displacement for different applied loads and crack extension.

For understanding this non-linear behavior, a tensile test is performed. Figures 13 (a) and (b) illustrated true stress-strain curve of PTFE polymer for quasi-static load, i.e., low strain-rate, and room temperature, considering large and small deformations, respectively. In order to predict the non-linear behavior of PTFE under tensile for small deformation the following classical mathematical model is proposed,

$$\sigma = \sigma_0\left[1 - \exp(-\beta\varepsilon)\right] \tag{9}$$

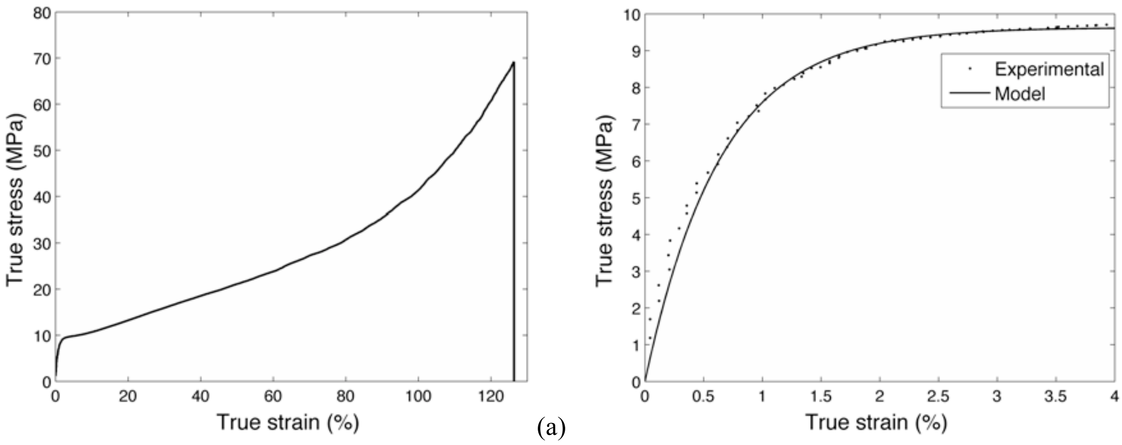

(a) (b)

Figure 13. Stress-strain curve for low strain-rate and room temperature: (a) large deformation and (b) small deformation.

By fitting Eq. (9) to the experimental data, the parameters σ_0 = 9.63 MPa and β = 1.55 are estimated. In present analysis σ_0 is larger than yield stress. Observing the uniaxial stress-strain response in Fig 13 (b) and comparing the amplitude parameter σ_0 with values presented in Tab. 1, it is noted that the values of stress less than 7MPa the nonlinear behavior is less significant.

5. CONCLUSION

In the present work full-field displacements around a crack of PTFE specimen were investigated. In order to this, an expression based on classical linear fracture mechanic was used to fit the experimentally measured displacement fields. Full-field displacements were obtained by means of digital image correlation method. By results, the nonlinear behavior increases for stress values larger than 7MPa. For future work the author aim to approach an expression that to take into account the nonlinear behavior of stress observed in tensile test.

6. ACKNOWLEDGEMENTS

The financial support of Rio de Janeiro State Funding, FAPERJ, and Research and Teaching National Council, CNPq, are gratefully and acknowledged.

7. REFERENCES

Avril, S, Bonnet, M, Bretelle, AS, Grédiac, M, Hild, F, Ienny, P, Latourte, F, Lemosse, D. Pagano, S, Pagnacco, E and Pierron, F Overview of Identification Methods of Mechanical Parameters Based on Full-field Measurements. Exp Mech 2008; 48:381–402.

Bergström, JS and Hilbert, LB, A constitutive model for predicting the large deformation thermomechanical behavior of fluoropolymers. Mech Mat; 2005 37:899–913.

Chen, J, Zhang, X, Zhan, N and Hu, X, Deformation measurement across crack using two-step extended digital image correlation method. Opt Lasers Eng 2010; 48:1126–1131.

Dally, JW and Riley, WF, Experimental Stress Analysis, 4th ed. McGraw Hill, 2005.

Dournaux, JL Bouvier, S, Aouafi, A and Vacher, P, Full-field measurement technique and its application to the analysis of materials behaviour under plane strain mode. Mat Sci Eng A 2009; 500:47–62.

Guélon, T, Toussaint, E, Le Cam, JB, Promma N and Grédiac, M, A new characterisation method for rubber. Polym Test 2009; 28:715–723.

Gdoutos, EE, Fracture Mechanics: *An Introduction*, 2nd Ed., Springer, 2005.

Huang, J, Pan, X, Peng, X, Zhu, T, Qin, L, Xiong, C and Fang, J, High-efficiency cell–substrate displacement acquisition via digital image correlation method using basis functions. Opt Lasers Eng 2010; 48:1058–1066.

Lava, P., Coppieters, S., Wang, Y., Van Houtte, P., Debruyne, D., Error estimation in measuring strain fields with DIC on planar sheet metal specimens with a non-perpendicular camera alignment,Optics and Lasers in Engineering 2011;49 (1):57-65.

Lava, P., Cooreman, S., Debruyne, D., Study of systematic errors in strain fields obtained via DIC using heterogeneous deformation generated by plastic FEA, Optics and Lasers in Engineering 2010;48 (4):457-468.

Nunes, LCS Mechanical characterization of hyperelastic polydimethylsiloxane by simple shear test. Materials Science and Engineering A 528 (2011) 1799–1804.

Nunes, LCS, Mechanical characterization of polytetrafluoroethylene polymer using full-field displacement method (doi:10.1016/j.optlaseng.2011.01.011).

Poissant, J and Barthelat, F, A Novel "Subset Splitting" Procedure for Digital Image Correlation on Discontinuous Displacement Fields. Exp Mech 2010; 50:353–364.

Pan, B, Asundi, A, Xie, H and Gao, J, Digital image correlation using iterative least squares and pointwise least squares for displacement field and strain field measurements. Opt Lasers Eng 2009; 47:865–874.

Roux, S, Réthoré, J and Hild, F, Digital image correlation and fracture: an advanced technique for estimating stress intensity factors of 2D and 3D cracks, J. Phys. D: Appl. Phys. 2009 42:214004 (21pp)

Rae, PJ and Dattelbaum, DM, The properties of poly(tetrafluoroethylene) (PTFE) in compression. Polymer 2004; 45:7615–7625.

Rae, PJ and Brown, EN, The properties of poly(tetrafluoroethylene) (PTFE) in tension, Polymer 2005 46:8128–8140.

Sharpe, WN, Handbook of Experimental Solid Mechanics, Springer Science and Business Media, LLC New York. 2008.

Triconnet, K, Derrien, K, Hild, F and Baptiste, D, Parameter choice for optimized digital image correlation. Opt Lasers Eng 2009; 47: 728–737.

Yoneyama, S, Ogawa, T and Kobayashi, Y, Evaluating mixed-mode stress intensity factors from full-field displacement fields obtained by optical methods. Eng Fract Mech 2007; 74:1399–1412.

Yates, JR, Zanganeh, M, Tai, YH, Quantifying crack tip displacement fields with DIC. Eng Fract Mech 2010; 77: 2063–2076.

Zhang, J., Cai, Y., Ye, W., Yu, T.X., On the use of the digital image correlation method for heterogeneous deformation measurement of porous solids, Optics and Lasers in Engineering 2011;49(2):200-209.

8. RESPONSIBILITY NOTICE

The author is the only responsible for the printed material included in this paper.